

New Method for Verification of Analytical Device Models Using Transistor Parameter Fluctuations

Christian Kühn¹, Stephan Marksteiner², Thomas E. Kopley^{2,3}
and Werner Weber²

¹Institute of Electronics, ET4, Universität der Bundeswehr, D-85577 Neubiberg, Germany

²Siemens AG, ZT ME, D-81730 Munich, Germany,

³now with Hewlett-Packard Company, Palo Alto, CA

Abstract

In this work device parameter fluctuations are considered for verification of analytical device models. We focus on the $(WL)^{-1/2}$ -dependence of the standard deviation of the threshold voltage σ_{V_T} [1-6]. Besides the known contribution from doping variations, an explicit channel length dependence enhances substantially the $(WL)^{-1/2}$ -curve. Oxide thickness variation is shown to have minor influence on the V_T -fluctuation and the contribution of mobility fluctuation is completely negligible for a 0.5 μm process. It has been found that a percolation model [13] for the current paths through the device can give full account of the experimentally measured values of σ_{V_T} .

Surface Channel n-MOSFET

In general, for a V_T -model which is a function of different statistically independent parameters p_i , $\sigma_{V_T}^2$ can be expressed as the sum of the squared standard deviations σ_{V_T, p_i}^2 of the corresponding parameters p_i :

$$V_T = V_T(p_1, \dots, p_n) \rightarrow \sigma_{V_T}^2 = \sum_{i=1}^n \left(\frac{\partial V_T}{\partial p_i} \right)^2 \cdot \sigma_{p_i}^2, \quad (1)$$

The following simple V_T -model is commonly used for the n-MOSFET [7]:

$$V_T = V_{FB} + \Psi_B + \frac{\sqrt{2\epsilon_0\epsilon_{Si}qN_A\Psi_B}}{C_{Ox}} + \frac{qD_i}{C_{Ox}}, \quad (2)$$

where V_{FB} is the flat-band-voltage, Ψ_B the surface potential at the onset of strong inversion, N_A the bulk doping, D_i the threshold adjust implant dose and C_{Ox} the gate oxide capacitance per unit area.

The analytical calculation of the standard deviation σ_{V_T} yields for the surface channel n-MOSFET [1]:

$$\sigma_{V_T, doping} = \frac{1}{C_{Ox}} \sqrt{\left(\frac{qQ_B}{4} + q^2 D_i \right)} \cdot \frac{1}{\sqrt{WL}}, \quad (3)$$

where Q_B is the depletion layer charge density and WL the effective gate area.

Equation (3) suffers from two shortcomings: first, the usual method for determining D_i is to apply a certain bulk doping level N_A (determined e.g. from SIMS data) and then to fit D_i in order to reproduce the measured long-channel value of V_T . This leads to an ambiguity in the value of the parameter D_i , and thus to an uncertainty in σ_{V_T} according to (3). As an example, we use the doping profile of the n-MOSFET of a 0.5 μm process [5] given in Fig. 1. Using the measured value of N_A and fitted value of D_i (to obtain the correct long-channel V_T) approximately 80 % of the experimental V_T

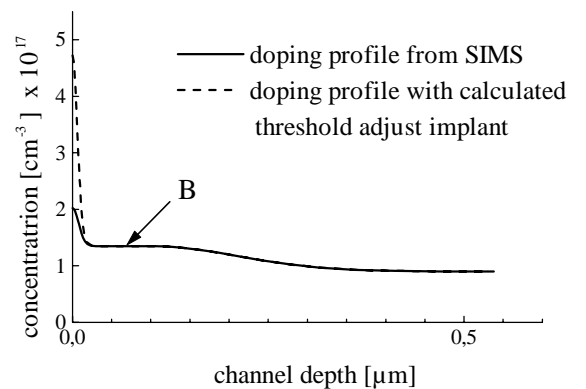


Figure 1: Doping profile for the NMOS surface channel determined by SIMS. The fitted doping value from the long-channel V_T is marked by a dotted line.

variations is explained. However, the calculated D_i is found to be largely exaggerated as compared to the SIMS profile (Fig.1).

On the other hand, optimizing N_A and D_i so that the SIMS profile is well represented yields for devices with different W and L geometries a σ_{V_T} that is only about 50% of the measured value (Fig. 2).

This result is furthermore confirmed by two-dimensional MEDICI simulations using the exact profile in Fig.1, which are in good agreement with the more refined 2D simulation method by Stolk and Klaassen [4]. There, the local variation of the doping concentration is considered dividing a cut through the device into cells and using a Poisson distribution for the number of dopants in each cell.

The second shortcoming of (3) is that it cannot account for the channel-length dependence of σ_{V_T} [8] shown in Fig. 3. Here, the short-channel devices show considerably larger σ_{V_T} 's (for the same $W \times L$) than the long channel n-MOSFETs. An explanation of this effect can be based on a more sophisticated V_T -model [9] which considers short channel effects:

$$V_T = V_{T0} - \eta(2\Phi_{bi} + U_{DS});$$

$$\eta = \frac{6T_{Ox}}{x_d} \cdot \exp\left(-\frac{\pi L}{4x_d}\right). \quad (4),$$

where V_{T0} is the threshold voltage of the long channel device, Φ_{bi} the built-in-voltage of the p-n-junction between source/drain and the channel, T_{Ox} the oxide thickness, x_d the depth of the space charge layer and L the effective channel length. The values of σ_{V_T} resulting from this refined model are also shown in Fig. 3. The channel length effect is clearly visible and the separation of the two branches is in good agreement with the experiment. It can thus be concluded that this channel length effect comes from the reduction of the effective channel length due to the source and drain depletion layers as modeled in (4). However, there is still a difference

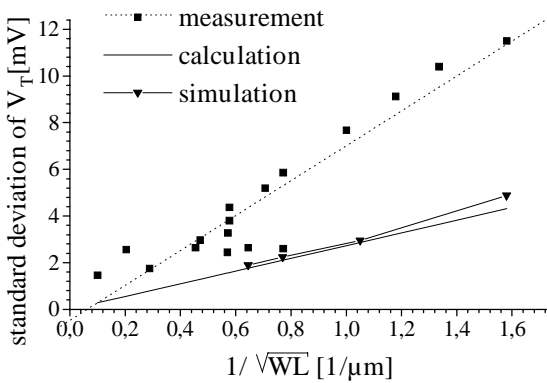


Figure 2: NMOS surface channel: Standard deviation of the threshold voltage vs. $(WL)^{-1/2}$ for different W and L geometries: Measurement, MEDICI simulation and analytically calculated values, following (1), show that direct contribution from the doping variations can explain 50% of the total variation.

of approximately 50% between experimental and theoretical data.

Let us now turn to the discussion of additional sources for the variation of V_T that can account for the remaining 50%.

Variations of the oxide thickness are investigated in [10] by AFM (atomic force microscopy) stating a rms surface roughness $\Delta=0.3nm$ of the oxide and its correlation length $L_c=15nm$.

In order to estimate the influence of oxide thickness variations on the V_T -fluctuation a simplification that is comparable to the one that leads to (3) is used. There, the doping is treated as homogenous for the whole device, neglecting local fluctuations.

Thus an average of the oxide thickness and its standard deviation σ_d is calculated with the use of Δ and L_C :

$$\sigma_d^2 = 2 L_C^2 \Delta^2 \cdot \frac{1}{WL} \quad (5).$$

The factor 2 originates from the assumption that the roughness of both the Si/SiO₂ interface and the SiO₂/gate interface are equal as reported in [11].

Combining the above equation with (1) and (2) leads to an influence of oxide thickness variation on σ_{V_T} of:

$$\sigma_{V_T, T_{Ox}} = \frac{Q_B + qD_i}{\epsilon_0 \epsilon_{Si}} \sqrt{2} L_C \Delta \cdot \frac{1}{\sqrt{WL}} \quad (6).$$

Using again the data of our 0.5 μm process, the contribution of $\sigma_{V_T, T_{Ox}}$ to the total threshold variation σ_{V_T} is found two orders of magnitude smaller than $\sigma_{V_T, doping}$, which confirms the observation by Mizuno [2] concerning the independence of σ_{V_T} from oxide thickness variation.

Calculations of $\sigma_{V_T, \mu}$ due to fluctuations of the mobility are based on the comprehensive mobility model in [12], where the mobility $\mu(E_T)$ in the inversion layer is determined as a function of the transverse electric field. A requirement for the validity of this model is that the device dimensions are large

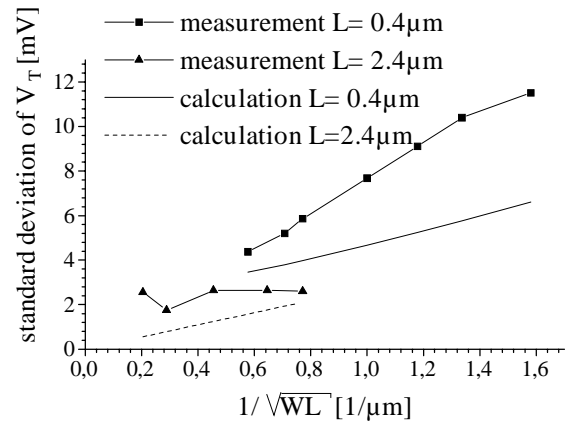


Figure 3: NMOS surface channel: Standard deviation of the threshold voltage vs. $(WL)^{-1/2}$ for devices with two different channel lengths: Measurement and calculated values show an additional dependence on the gate length, whereas the 50% disparity between experiment and theory still exists.

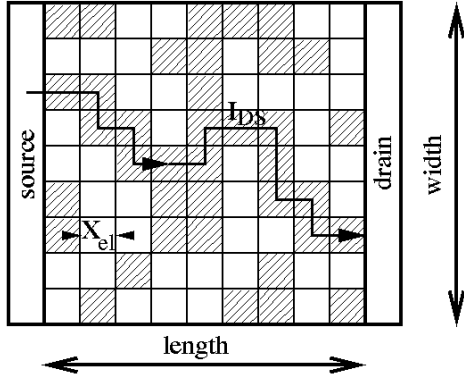


Figure 4: Schematic top view of the oxide - semiconductor interface plane: Due to local inhomogeneities of the doping the surface potential of some parts of the interface has already reached the strong inversion (hatched squares) whereas others are still in the state of weak inversion (blank squares). Depending on the local distribution of the inverted areas percolation paths through the device can appear.

enough to establish an effective carrier mobility from the ensemble averaging of single scattering processes, which is true for the 0.5 μm process. The transverse electric field depends on the doping concentration and is thus a fluctuating parameter. A lengthy calculation shows that for a fixed oxide charge density of $2 \times 10^{10} \text{ cm}^{-2}$ the contribution from $\sigma_{V_{t,\mu}}$ is several orders of magnitude smaller than $\sigma_{V_{t,\text{doping}}}$.

All existing calculations of parameter fluctuations suffer from neglecting the full three-dimensional character of the problem. Percolation occurs due to the spatial variation of the distribution of doping atoms which causes local potential fluctuations at the interface between semiconductor and gate oxide (Fig. 4). This leads to variations in the current paths in the device. An analytic approximation in [13] subdivides the gate area into square elements and assumes those either as conducting or non-conducting. On this basis a formula for σ_{V_t} is derived:

$$\sigma_{V_{t,perc}} = \sqrt{\frac{\pi}{2}} \left(\frac{WL}{x_{el}^2} \right)^{-3/8} \cdot \sigma_{V_{t,el}}, \quad (7)$$

where x_{el} is the length of the square subdivisions of the gate area and $\sigma_{V_{t,el}}$ is the standard deviation of threshold voltage for a subdivision square. Assuming a normal distribution for the doping in each subdivision square leads to:

$$\sigma_{V_{t,perc}} = \sqrt{\frac{\pi}{2}} \cdot \frac{q}{2C_{Ox}} \sqrt{N_A x_d} \cdot x_{el}^{-1/4} \cdot (WL)^{-3/8} \quad (8)$$

where x_d is the depth of the space charge layer below the gate.

For the length of the subdivisions two different values have been used, the depth of the space charge layer, as proposed in [13], and the Debye length, as a typical length for the influence of a potential perturbation in the semiconductor.

Fig. 5 shows the results of these calculations together with the experimental data. As the percolation model has a digital

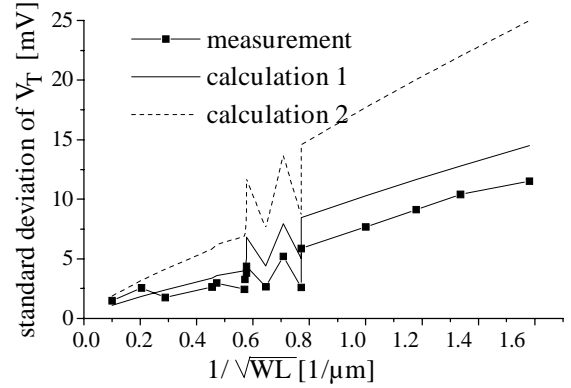


Figure 5: NMOS surface channel: Standard deviation of the threshold voltage vs. $(WL)^{-1/2}$ for different W and L geometries: Measurement (squares) and calculated standard deviations of V_T derived from the percolation model in [13] including channel length effects, with two different values for the size of the subdivision of the gate area. The subdivision length is chosen to be the depth of the space charge layer (calculation 1) and to be the Debye length (calculation 2).

character and thus neglects subthreshold characteristics, it leads to calculated values that are higher than the actually measured ones. We conclude that a percolation model for the current in the subthreshold region can indeed account for the remaining 50% between experimental and theoretical values in Fig. 2.

Buried Channel p-MOSFET

Let us now turn to the buried-channel p-MOSFET, where a similar derivation of the V_T -variation was carried out:

$$\sigma_{V_T}^2 = \left(\frac{\partial V_T}{\partial N_p} \right)^2 \cdot \sigma_{N_p}^2 + \left(\frac{\partial V_T}{\partial N_n} \right)^2 \cdot \sigma_{N_n}^2, \quad (9)$$

$$\sigma_{N_i}^2 = \frac{N_{Ai} + N_{Di}}{x_i} \cdot \frac{1}{WL}, \quad (10)$$

where N_p and N_n are the net doping concentrations of the p- and the n-region, N_{Ai} and N_{Di} are the actual acceptor and donor concentrations and x_i is the depth of the space charge layer in the respective region

This general formula is applied to the different V_T -models proposed by Sze [7], Van der Tol [14] and Klaassen [15]. The model of Van der Tol can be converted into the one suggested by Nishiuchi [16] and adopted by Sze.

For our calculations on the p-MOSFET, values for the average doping concentrations are again taken from SIMS data (Fig. 6). The calculated standard deviations of the threshold voltage according to (9) and (10) using Sze's formula cannot be brought into agreement with the 50% disparity between experiment and corresponding simple theory (3) for the NMOS, that assumes an overall distribution for the quantity of dopant atoms. The contributions to the standard deviation from additional effects as discussed above

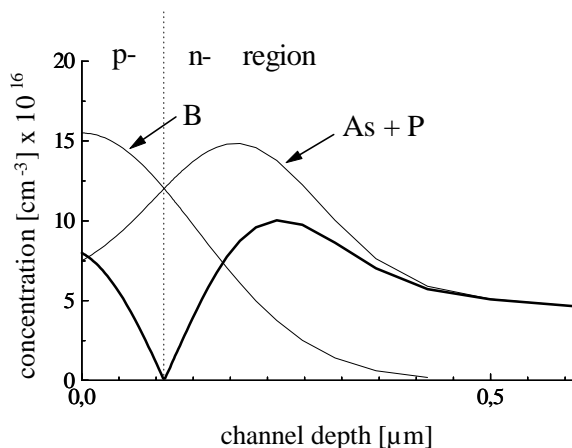


Figure 6: Doping profile for the PMOS buried channel device determined by SIMS.

and especially from percolation considerations also exist for the PMOS buried channel with a similar proportion as for the NMOS.

For the PMOS another additional contribution exists: the variation of the position of the junction between the p-doped and the n-doped channel regions, which will increase the standard deviation by about 15%.

Klaassen suggested a V_T -model that accounts for the two different operation modes of the buried channel p-MOSFET. These operation modes are characterized by the location where conduction first appears, i.e. whether the carriers are generated directly at the oxide-semiconductor interface or at some distance away from it.

Applying (1) to his V_T -formula we get values for the standard deviation from the direct influence of doping fluctuations without consideration of percolation effects and channel length effects, that reach about 50% of the experimental data similar to the NMOS case. In Fig. 7 the results of these calculations are shown together with the theoretical curves for the percolation model applied to the PMOS case.

In conclusion the PMOS model of Klaassen leads to good agreement between our theoretical considerations and the experimental data and is thus more favorable than that of Sze. This demonstrates, that device models can be tested based on the measurement of device parameter variations.

Acknowledgment

The authors wish to thank K. Hoffmann (Universität der Bundeswehr) for his contribution to this work. This work was supported by the DFG (Ho 1325/2-2).

References

[1] K. Lakshmikummar, R. Hadaway and M. Copeland, 'Characterization and Modeling of Mismatch in MOS Transistors for Precision Analog Design', *IEEE J. of Solid State Circuits* 21, pp. 1057-1066, 1986.

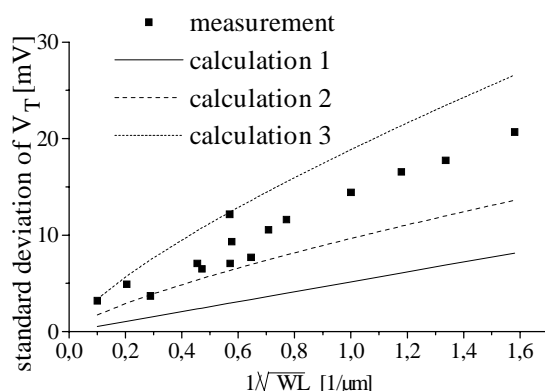


Figure 7: PMOS buried channel: Standard deviation of the threshold voltage vs. $(WL)^{-1/2}$: Measurement (squares) and calculations based on the V_T -model by Klaassen [15], the solid line shows the calculations acc. to (9) and (10) that account only for homogenous doping variation and the dashed lines show the calculations from the percolation model with two subdivision lengths: the Debye length (calculation 2) and the depth of the space charge layer (calculation 3).

[2] T. Mizuno, J. Okamura and A. Toriumi, 'Experimental Study of Threshold Voltage Fluctuation Due to Statistical Variation of Channel Dopant Number in MOSFET's', *IEEE Trans. Electron Dev.* 41, pp. 2216-2221, 1994.

[3] T. Mizuno, 'Influence of Statistical Spatial-Nonuniformity of Dopant Atoms on Threshold Voltage in a System of Many MOSFET's', *Jpn. J. Appl. Phys.* 35, pp. 842-848, 1996.

[4] P.A. Stolk and D.B.M. Klaassen, 'The Effect of Statistical Fluctuations on MOS Device Performance', *IEDM Tech. Dig.*, pp. 627-630, 1996.

[5] M. Eisele et al., 'Intra-Die Device Parameter Variations and Their Impact on Digital CMOS Gates at Low Supply Voltages', *IEDM Tech Dig.*, pp. 67 - 70, 1995.

[6] C. Kühn and W. Weber, 'A new Method for Verification of MOSFET Models Based on Device Parameter Variations', *ESSDERC 1997*, in press

[7] S.M. Sze, *Physics of Semiconductor Devices*, Wiley, New York, p. 467, 1981.

[8] M. Steyaert et al., 'Threshold Voltage Mismatch in Short Channel MOS Transistors', *Electronics Letters* 30, pp. 1546-1547, 1994

[9] K. Ratnakumar and J. Meindl, 'Short Channel MOST Threshold Voltage Model', *IEEE J. of Solid State Circuits* 17, pp. 937-948, 1982.

[10] T. Yoshinobu, A. Iwamoto and H. Iwasaki, 'Scaling Analysis of SiO₂/Si Interface Roughness by Atomic Force Microscopy', *Jpn. J. Appl. Phys.* 33, pp. 383-388, 1994.

[11] T. Ohmi, M. Miyashita, M. Itano, T. Imaoka and I. Kawanabe, 'Dependence of Thin-Oxide Films Quality on Surface Microroughness', *IEEE Trans. Electron Dev.* 39, pp. 537-545, 1992.

[12] S. Schwarz and S. Russek, 'Semi-Empirical Equations for Electron Velocity in Silicon: Part II - MOS Inversion Layer', *IEEE Trans. Electron Dev.* 30, pp. 1634-1639, 1983.

[13] R. Keyes, 'The Effect of Randomness in the Distribution of Impurity Atoms on FET Thresholds', *Appl. Phys* 8, pp. 251-259, 1975

[14] M. Van der Tol and S. Chamberlain, 'Potential and Electron Distribution Model for the Buried Channel MOSFET', *IEEE Trans. Electron Dev* 36 pp. 670-689, 1989.

[15] F.M. Klaassen and W. Hes, 'Compensated MOSFET Devices', *Solid State Electronics* 28, pp. 359-373, 1985.

[16] K. Nishiuchi, H. Oka, T. Nakamura, H. Ishikawa and M. Shinoda, 'A Normally-Off Type Buried Channel MOSFET for VLSI Circuits', *IEDM Tech. Dig.*, pp. 26-29, 1978.